Supplementary Materials for

Independent Amplitude Control of Arbitrary Orthogonal States of Polarization via Dielectric Metasurfaces

Qingbin Fan[1,2], Mingze Liu[1,3], Cheng Zhang[4], Wenqi Zhu[5,6], Yilin Wang[1,3], Peicheng Lin[1,3], Feng Yan[2], Lu Chen[5,6], Henri J. Lezec[5], Yanqing Lu[1,3], Amit Agrawal[5,6] and Ting Xu[1,3]

1. *National Laboratory of Solid-State Microstructures, Jiangsu Key Laboratory of Artificial Functional Materials, Collaborative Innovation Center of Advanced Microstructures, Nanjing University, Nanjing 210093, China*
2. *School of Electronic Science and Engineering, Nanjing University, Nanjing 210093, China*
3. *College of Engineering and Applied Sciences, Nanjing University, Nanjing 210093, China*
4. *School of Optical and Electronic Information and Wuhan National Laboratory for Optoelectronics, Huazhong University of Science and Technology, Wuhan 430074, China.*
5. *Physical Measurement Laboratory, National Institute of Standards and Technology, Gaithersburg, MD 20877, USA*
6. *Maryland NanoCenter, University of Maryland, College Park, MD 20877, USA*

Ⅰ.DESIGN AND SIMULATION OF PERIODIC ARRAYS OF META-MOLECULES

As mentioned in the main text, the meta-molecule designs are based on the Jones matrix $J(x,y)$ in Eq. 5. We can extract the required phase shifts (φ_x, φ_y) and rotation angle θ of the dielectric unit from the eigenvalues and eigenvectors of the matrix. FIG. S1 and TABLE. S1 show the detailed structural parameters of the proposed meta-molecules. All the simulations shown in the main text are performed using a commercial finite-difference time-domain (FDTD) software with plane wave illumination from substrate for an infinitely periodic square arrays of the designed meta-molecules. In the simulations, periodic boundary conditions are employed at the *x* and *y* directions and perfectly matched layers (PML) at the *z* boundaries. The mesh size added on the meta-molecule is *dx* = *dy* = *dz* = 5 nm, which can ensure the accuracy of the calculated results. To obtain arbitrary polarized light, two orthogonal linearly polarized light sources with required phase difference and amplitude values are added in the simulation region.

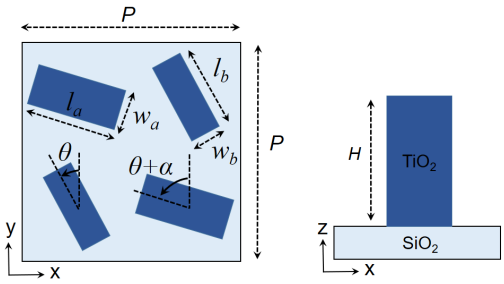

FIG. S1. Details of the meta-molecule. Each meta-molecule is composed of two pairs of twin elements with different birefringent properties to form a submicron interference system. The proposed meta-molecule is composed of rectangular titanium dioxide (TiO_2) nanopillars on a fused-silica substrate. The TiO_2 nanopillars are designed to have identical heights of *H*=600 nm and organized in a square array with a lattice constant of *P* = 360 nm.

Table. S1. The meta-molecule designs for the demonstration of dichroism. LP: linear polarization. CP: circular polarization. EP: elliptical polarization.

	LP	CP	EP
Element 1	l_a=145 nm w_a=145 nm	l_a=100 nm w_a=265 nm	l_a=190 nm w_a=100 nm
Element 2	l_b=293 nm w_b=117 nm	l_b=125 nm w_b=305 nm	l_b =125 nm w_b =220 nm

There are two possible arrangements (staggered and parallel) for a pair of twin-meta-atoms in a meta-molecule, as shown in Fig. S2. According to numerical simulations, these two arrangements offer similar amplitude response. The reason we choose staggered arrangement (Fig. S2 (a)) in our design is because compared to the parallel arrangement, the staggered case is easier to fabricate. For example, in some cases (as shown in Fig. S2(e)), the edge-to-edge distance between two neighboring meta-atoms in the parallel arrangement is much smaller than that can be achieved using state-of-the-art electron beam lithography techniques employed here for nanofabrication.

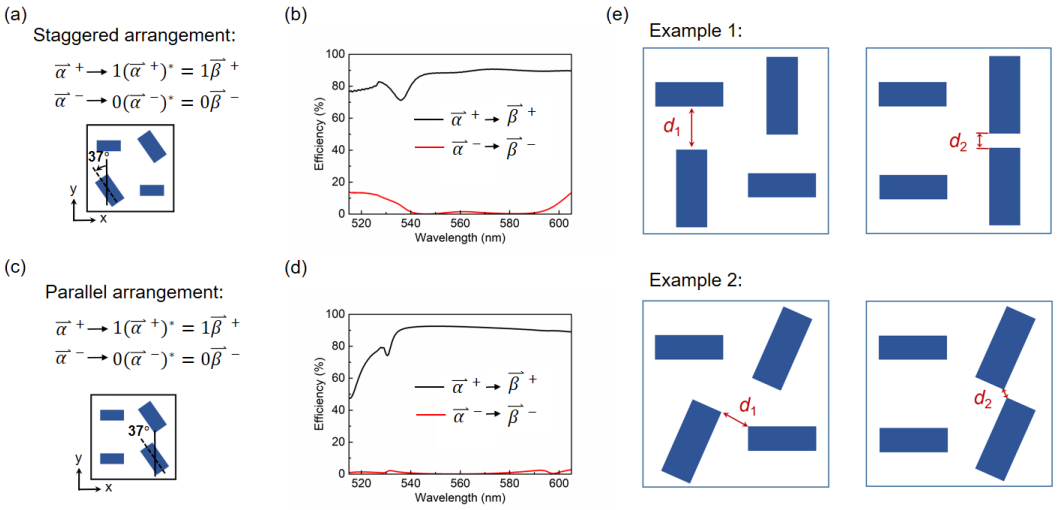

Figure. S2. Dichroism of orthogonal, elliptical polarization states (δ=π/3, χ=π/6) in a meta-molecule system. The polarization conversion spectrum for the meta-molecule system with (a-b) staggered arrangement and (c-d) parallel arrangement. (e) Comparison of two possible nanostructures arrangements to form a square meta-molecule.

Ⅱ : DERIVATION OF THE JONES MATRIX J AND ITS EIGENVALUES AND EIGENVECTORS FOR CIRCULAR POLARIZATION STATES

In this section, we emphasize only the relationship between amplitude and circular polarization states. Assume that the metasurface should impart two independent amplitude profiles, $|U^+(x,y)|$ and $|U^-(x,y)|$, on input circular polarization states $\{|\mathrm{R}\rangle, |\mathrm{L}\rangle\}$. As mentioned in the main text, the relationship between the input and output polarization states is complex conjugate. It means that the output polarization states have the same states as the input states with flipped handedness. Such meta-device can be expressed by Jones matrix $J(x,y)$ that simultaneously satisfies:

$$J(x,y)\,|R\rangle = e^{if^{-1}(|U^+(x,y)|)}|L\rangle \ , \tag{S1}$$

$$J(x,y)\,|L\rangle = e^{if^{-1}(|U^-(x,y)|)}|R\rangle \ . \tag{S2}$$

Upon matrix inversion of Eq. S1 and S2, the Jones matrix $J(x,y)$ can be expressed as

$$J(x,y) = \begin{bmatrix} e^{if^{-1}(|U^+(x,y)|)} & e^{if^{-1}(|U^-(x,y)|)} \\ -ie^{if^{-1}(|U^+(x,y)|)} & ie^{if^{-1}(|U^-(x,y)|)} \end{bmatrix} \begin{bmatrix} 1 & 1 \\ i & -i \end{bmatrix}^{-1} \tag{S3}$$

After calculation and simplification, the matrix $J(x,y)$ has the form:

$$J(x,y) = \frac{1}{2}\begin{bmatrix} e^{if^{-1}(|U^+(x,y)|)} + e^{if^{-1}(|U^-(x,y)|)} & ie^{if^{-1}(|U^-(x,y)|)} - ie^{if^{-1}(|U^+(x,y)|)} \\ ie^{if^{-1}(|U^-(x,y)|)} - ie^{if^{-1}(|U^+(x,y)|)} & -e^{if^{-1}(|U^+(x,y)|)} - e^{if^{-1}(|U^-(x,y)|)} \end{bmatrix} \tag{S4}$$

This matrix provides a general form of switching between two independent amplitude profiles for circular polarization incident light. To understand the working principle of the meta-device more intuitively, we present the expression that relates output and input polarization light as $|E_{out}\rangle = J|E_{in}\rangle$. Here, incident light $|E_{in}\rangle$ is one of the two orthogonal, circular polarization states. The expansion of the output matrix has the form:

$$|E_{out}\rangle = \frac{1}{2}\begin{bmatrix} e^{if^{-1}(|U^+(x,y)|)} + e^{if^{-1}(|U^-(x,y)|)} & ie^{if^{-1}(|U^-(x,y)|)} - ie^{if^{-1}(|U^+(x,y)|)} \\ ie^{if^{-1}(|U^-(x,y)|)} - ie^{if^{-1}(|U^+(x,y)|)} & -e^{if^{-1}(|U^+(x,y)|)} - e^{if^{-1}(|U^-(x,y)|)} \end{bmatrix} \begin{bmatrix} 1 \\ i \end{bmatrix}$$

$$= \frac{1}{2}\begin{bmatrix} 2e^{if^{-1}(|U^+(x,y)|)} \\ -2ie^{if^{-1}(|U^+(x,y)|)} \end{bmatrix}$$

$$= e^{if^{-1}(|U^+(x,y)|)}\begin{bmatrix} 1 \\ -i \end{bmatrix} \tag{S5}$$

The device has generated the targeted amplitude profile and expected polarization state. We can come to the same conclusions for the orthogonal state. By calculating the matrix $J(x,y)$, we can obtain the eigenvalues as

$$\xi_1 = e^{i[\frac{1}{2}(f^{-1}(|U^+(x,y)|)+f^{-1}(|U^-(x,y)|)]} , \tag{S6}$$

$$\xi_2 = e^{i[\frac{1}{2}\left((f^{-1}(|U^+(x,y)|)+f^{-1}(|U^-(x,y)|)\right)-\pi]} , \tag{S7}$$

and eigenvectors as

$$|r_1\rangle = \begin{bmatrix} \cos\frac{1}{4}[\left(f^{-1}\left(\left|U^+(x,y)\right|\right) - f^{-1}(|U^-(x,y)|)\right)] \\ sin\frac{1}{4}[\left(f^{-1}\left(\left|U^+(x,y)\right|\right) - f^{-1}(|U^-(x,y)|)\right)] \end{bmatrix} , \tag{S8}$$

$$|r_2\rangle = \begin{bmatrix} -\sin\frac{1}{4}[\left(f^{-1}\left(\left|U^+(x,y)\right|\right) + f^{-1}(|U^-(x,y)|)\right)] \\ cos\frac{1}{4}[\left(f^{-1}\left(\left|U^+(x,y)\right|\right) + f^{-1}(|U^-(x,y)|)\right)] \end{bmatrix} . \tag{S9}$$

Since $|r_1\rangle$ and $|r_2\rangle$ are linearly independent vectors, the Jones matrix $J(x,y)$ can be transformed into canonical form $J = P\Lambda P^{-1}$, where P is an invertible matrix and Λ is a diagonal matrix. The expansion of the canonical form can be expressed as

$$J(x,y) = \mathrm{P}\Lambda\mathrm{P}^{-1} = \begin{bmatrix} \cos\frac{1}{4}[F(U^+) - F(U^-)] & -\sin\frac{1}{4}[F(U^+) - F(U^-)] \\ sin\frac{1}{4}[F(U^+) - F(U^-)] & cos\frac{1}{4}[F(U^+) - F(U^-)] \end{bmatrix}\cdots$$

$$\begin{bmatrix} e^{i[\frac{1}{2}(F(U^+)+F(U^-))]} & 0 \\ 0 & e^{i[\frac{1}{2}(F(U^+)+F(U^-))-\pi]} \end{bmatrix}\begin{bmatrix} \cos\frac{1}{4}[F(U^+) - F(U^-)] & -\sin\frac{1}{4}[F(U^+) - F(U^-)] \\ sin\frac{1}{4}[F(U^+) - F(U^-)] & cos\frac{1}{4}[F(U^+) - F(U^-)] \end{bmatrix} \tag{S10}$$

Here, $F(U^+)$ and $F(U^-)$ represent $f^{-1}(|U^+(x,y)|$ and $f^{-1}(|U^-(x,y)|$, respectively. Since the Jones matrix of the meta-device operates on linear polarization basis, we can easily

obtain the required phase shifts and rotation angles as a function of amplitude value

$$\varphi_x(x,y) = \frac{1}{2}[f^{-1}(|U^+(x,y)|) + f^{-1}(|U^-(x,y)|)], \quad \text{(S11)}$$

$$\varphi_y(x,y) = \frac{1}{2}[f^{-1}(|U^+(x,y)|) + f^{-1}(|U^-(x,y)|)] - \pi \ , \quad \text{(S12)}$$

$$\theta(x,y) = \frac{1}{4}[f^{-1}(|U^+(x,y)|) - f^{-1}(|U^-(x,y)|)] \ . \quad \text{(S13)}$$

Ⅲ: NANOFABRICATION OF TiO_2 METASURFACE

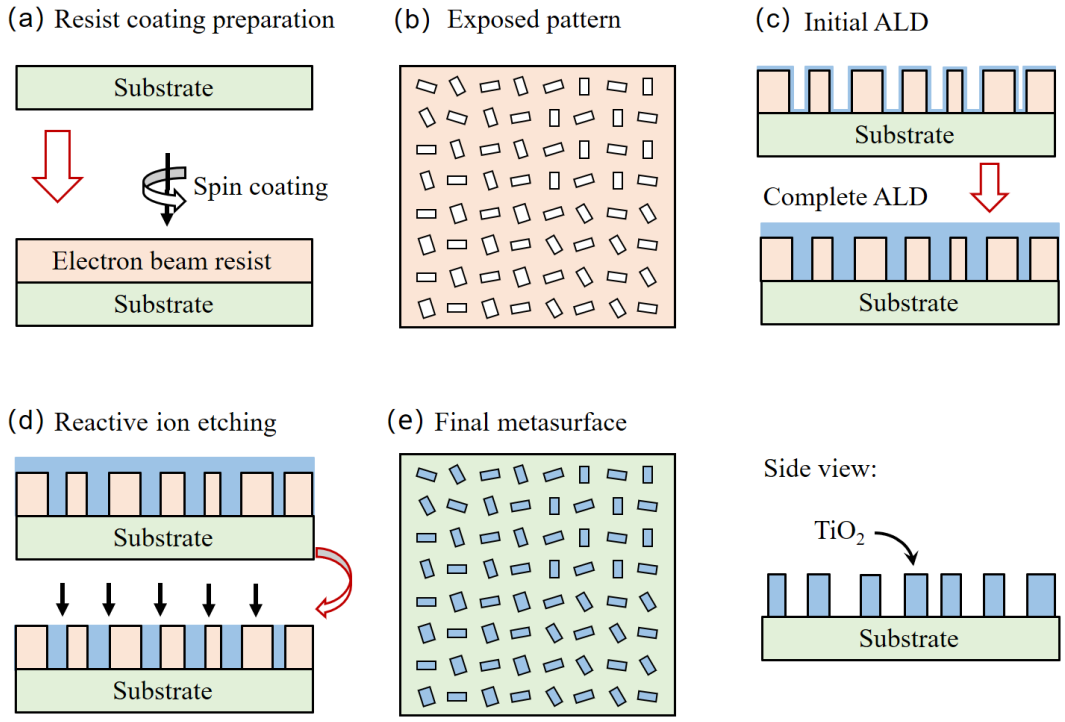

FIG. S3. Schematic illustrate of the metasurface fabrication. (a) Spin-coated photoresist. A double-side polished fused silica substrate was prime-vapor-coated with a layer of hexamethyldisilazane (HMDS) and then spin-coated with a layer of 600 nm thick, positive-tone electron beam resist (ZEP520A). (b) The e-beam lithography (EBL) is used to obtain the exposed pattern. This process was performed at an accelerating voltage of 100 kV and beam current of 2 nA. Then, the sample was developed in hexyl-acetate for two minutes. (c) Atomic layer deposition (ALD) process. The patterned sample was carried out the deposition of TiO_2. To avoid deformation of the resist pattern, the ALD chamber is set to 90 °C. (d) The over-coated TiO_2 layer was etched by the inductively-coupled-plasma reactive ion etching (ICP-RIE) in a mixture of Cl_2 and BCl_3 gas. The etching was

terminated when the over-coated TiO_2 had been completely removed and the resist was exposed. Finally, we removed the resist by soaking in n-methyl-2-pyrrolidone and produced the array of TiO_2 nanopillars with pre-designed geometries (e).

Ⅳ: SIMULATION OF METASURFACE NANOPRINTING FOR ANY PAIR OF ORTHOGONAL POLARIZATION STATES

In this section, we design and numerically simulate three metasurface arrays to demonstrate that our method can achieve two completely different nanoprinting patterns for any pair of orthogonal polarization states, including linear, circular, and elliptical polarization. Each metasurface array is designed to respectively generate two different character strings 'Meta' and 'Nano' for two orthogonal polarization states at the wavelength of 550 nm. Considering the calculation limit of the simulation workstation, the metasurface encoding these amplitude profiles is 36 μm × 108 μm in size and contain 50 × 150 meta-molecules. The simulation results are shown in Fig. S4. As expected, the metasurfaces present a pattern of 'Nano' characters with stereoscopic concave effect for one polarization state. When the incident light is switched to its orthogonal state, the metasurfaces exhibit a pattern of 'Meta' characters with totally different convex effect. These results are in good agreement with expectations and clearly demonstrate that independent amplitude control can be achieved for any pair of orthogonal polarization states. The rough image quality is mainly attributed to the small number of meta-molecules in the simulation. The corresponding metasurface arrays and feature sizes of TiO_2 nanopillars are shown in Fig. S5. and Table S2- S4, respectively.

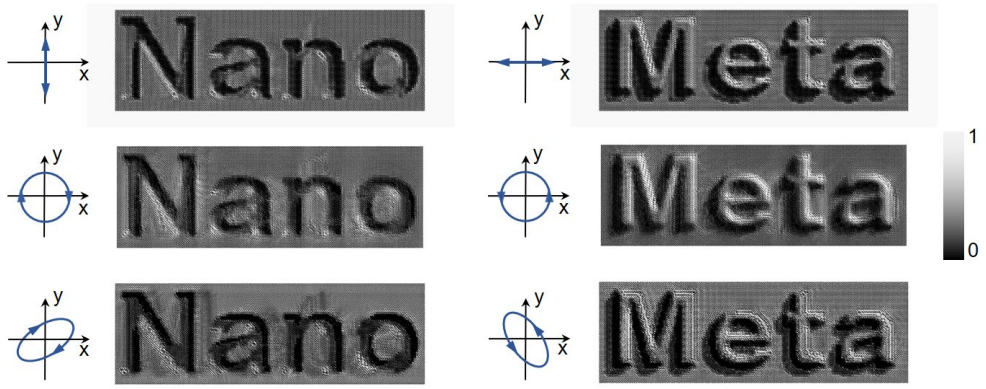

FIG. S4. Polarization-controllable nanoprinting to achieve two completely different transmitted images for any pair of orthogonal polarization states, including linear (δ=π/2, χ=π/2), circular (δ=π/2, χ=π/4), and elliptical polarizations (δ=π/3, χ=π/6). The metasurface encoding these amplitude profiles was 36 × 108 μm in size and contained 50 × 150 meta-molecules.

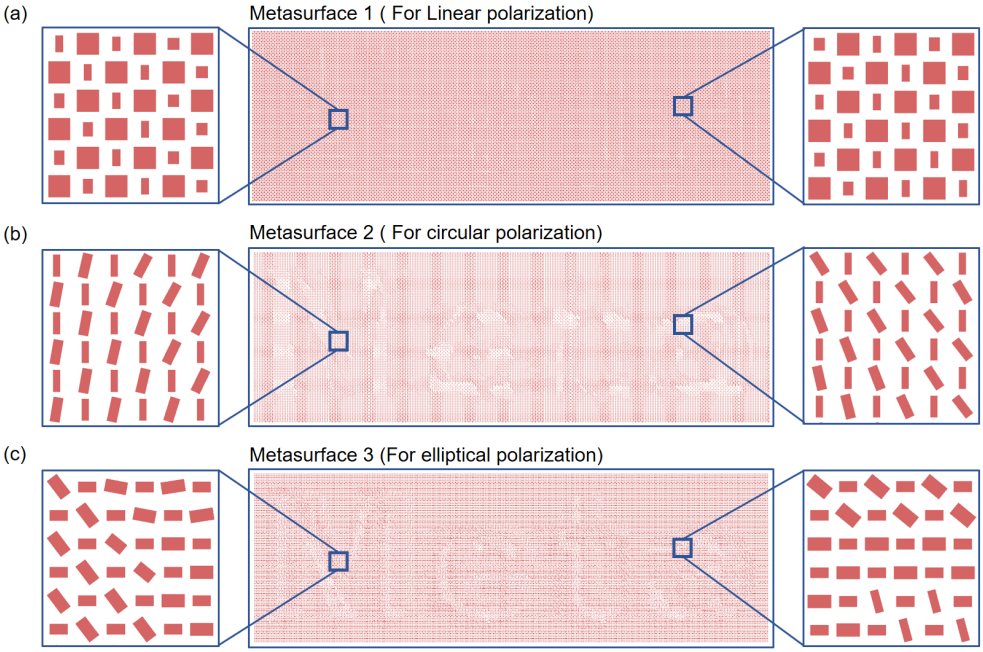

FIG. S5. The designed metasurface arrays used for (a) linear, (b) circular, and (c) elliptical polarizations. The left and right insets show a magnified view of the metasurface arrays (Top view).

Table S2. Feature sizes of TiO_2 nanopillars used for linear polarization.

	Unit cell				
No.	Length(nm)	Width (nm)	No.	Length(nm)	Width (nm)
1	280	280	15	140	155
2	180	180	16	145	145
3	155	185	17	120	215
4	163	163	18	125	185
5	140	200	19	130	170
6	145	175	20	130	160
7	155	155	21	135	150
8	135	200	22	140	140
9	140	175	23	90	275
10	145	165	24	100	210
11	150	150	25	105	185
12	125	220	26	105	180
13	135	175	27	110	165
14	140	160	28	110	155

Table S3. Feature sizes of TiO_2 nanopillars used for circular polarization.

	Unit cell				
No.	Length(nm)	Width (nm)	No.	Length(nm)	Width (nm)
1	90	275	5	120	300
2	100	270	6	125	320
3	110	280	7	315	65
4	115	295	8	275	80

Table S4. Feature sizes of TiO_2 nanopillars used for elliptical polarization

	Unit cell				
No.	Length(nm)	Width (nm)	No.	Length(nm)	Width (nm)
1	230	135	9	80	235
2	240	145	10	300	155
3	245	155	11	295	165
4	155	295	12	295	185
5	290	130	13	110	195
6	290	145	14	105	255
7	280	160	15	105	290
8	290	175	16	105	335